

# A passively Q-switched compact Er:Lu2O3 ceramics laser at 2.8 $\mu\text{m}$ with a graphene saturable absorber

journal or publication title	Applied Physics Express
volume	12
number	2
page range	022002
year	2019-01-10
URL	<a href="http://hdl.handle.net/10655/00012652">http://hdl.handle.net/10655/00012652</a>

doi: 10.7567/1882-0786/aaf994



## **Passively Q-switched Compact Er:Lu<sub>2</sub>O<sub>3</sub> Ceramics Laser at 2.8 μm with Graphene Saturable Absorber**

Hiyori Uehara<sup>1\*</sup>, Shigeki Tokita<sup>1\*</sup>, Junji Kawanaka<sup>1</sup>, Daisuke Konishi<sup>3</sup>, Masanao Murakami<sup>3</sup>, Ryo Yasuhara<sup>2\*</sup>

<sup>1</sup> *Institute of Laser Engineering, Osaka University, 2-6 Yamada-oka, Suita, Osaka 565-0871, Japan*

<sup>2</sup> *National Institute for Fusion Science, 322-6 Oroshi-cho, Toki 509-5292, Japan*

<sup>3</sup> *Mitsuboshi Diamond Industrial Co., Ltd., 32-12 Koroen, Settsu, Osaka 566-0034, Japan*

E-mail: uehara-h@ile.osaka-u.ac.jp, tokita-s@ile.osaka-u.ac.jp, yasuhara@nifs.ac.jp

We have demonstrated a passively Q-switched Er:Lu<sub>2</sub>O<sub>3</sub> ceramics laser using a monolayer graphene saturable absorber. Stable pulsed operation with watt-level average power was achieved by a compact linear cavity without focusing on the saturable absorber. This is the first demonstration of a passively Q-switched mid-IR Er:Lu<sub>2</sub>O<sub>3</sub> laser using a graphene saturable absorber. A maximum pulse energy of 9.4 μJ and a peak power of 33 W were achieved with a 247 ns pulse duration. To our knowledge, this is the shortest pulse duration, highest pulse energy, and highest peak power obtained with a graphene saturable absorber in the 3 μm wavelength region.

High-power mid-IR lasers with wavelengths of around 3  $\mu\text{m}$  have many potential applications in industry [1] and medicine [2] due to the strong absorption of these wavelengths by water.  $\text{Er}^{3+}$ -doped lasers are currently the most efficient way to obtain lasing in the 3  $\mu\text{m}$  wavelength region. Fluoride glass fiber is a suitable host material for Er lasers due to its low phonon energy. Er-doped ZBLAN fiber lasers with a continuous wave (CW) output of  $>20$  W [3-6] and a pulse energy of 100  $\mu\text{J}$  by  $Q$ -switching [7] have been reported. However, fluoride glass has disadvantages, including poor thermal properties, poor mechanical strength, and low moisture resistance, resulting in low laser durability. In addition,  $Q$ -switched pulse energy of a fiber laser will be limited by the core diameter. Er-doped cubic rare-earth sesquioxide crystals (e.g.,  $\text{Lu}_2\text{O}_3$ ,  $\text{Y}_2\text{O}_3$ , and  $\text{Sc}_2\text{O}_3$ ) are thus attracting attention as high-power mid-IR lasers due to their lower phonon energies and higher thermal conductivities compared with yttrium aluminum garnet (YAG). In particular,  $\text{Lu}_2\text{O}_3$  is a suitable host material because its thermal conductivity remains high even at high doping levels, due to the similar atomic masses and ionic radii of the  $\text{Lu}^{3+}$  and  $\text{Er}^{3+}$  ions. A maximum CW power of 5.9 W and a slope efficiency of 27% at 2.85  $\mu\text{m}$  have been reported for a 7 at.% Er-doped  $\text{Lu}_2\text{O}_3$  laser [8]. However, the fabrication of sesquioxide single crystals is generally difficult due to its high melting point of approximately 2490  $^\circ\text{C}$  and slow growth rate. High-quality polycrystalline transparent ceramics of the rare-earth sesquioxide, which have become available recently, open up the possibility of efficient high-power mid-IR lasers due to their advantageous mechanical strength and thermal properties compared with single crystals. Polycrystalline ceramics can also be mass produced cheaply as large-volume crystals.  $\text{Er}^{3+}$ -doped ceramics lasers with wavelengths at 2.8  $\mu\text{m}$  have been investigated in recent years. We have reported the highest CW output power of 2.3 W and a slope efficiency of 29% for high-quality Er: $\text{Lu}_2\text{O}_3$  ceramics [9,10], and detailed the optical properties of these ceramics with various doping concentrations. In the next stage, the Er-doped sesquioxides will be focused on with  $Q$ -switching to obtain much higher peak power. Numerous passively  $Q$ -switched Er: $\text{Lu}_2\text{O}_3$  lasers at mid-IR have recently been reported using a semiconductor saturable absorber mirror (SESAM) [11],  $\text{MoS}_2$  [12], black phosphorus [13], and graphitic carbon nitride [14] as saturable absorbers (SAs). Graphene film, which exhibits wavelength-independent characteristics and saturable absorption, is expected to become a promising saturable absorber for passive  $Q$ -switching or mode-locking of mid-IR lasers. Graphene was

also recently used for passive  $Q$ -switching of mid-IR lasers at around 3  $\mu\text{m}$ , e.g., Er:Y<sub>2</sub>O<sub>3</sub> ceramics laser [15], Er:ZBLAN fiber laser [16], Er:CaF<sub>2</sub> [17], Er:Pr:GGG [18], and Ho:Pr:LiLuF<sub>4</sub> [19].

In this work, we demonstrate a passively  $Q$ -switched Er:Lu<sub>2</sub>O<sub>3</sub> ceramics laser using a monolayer graphene SA. Stable pulsed operation was observed in a compact linear cavity without focusing on the SA. A maximum pulse energy of 9.4  $\mu\text{J}$  and peak power of 33 W were achieved with a pulse duration of 250 ns. This is the first demonstration of a passively  $Q$ -switched mid-IR Er:Lu<sub>2</sub>O<sub>3</sub> laser using a graphene SA.

An 11 at.% Er-doped Lu<sub>2</sub>O<sub>3</sub> polycrystalline transparent ceramics (Konoshima Chemical Co., Ltd.) without coating was used. An efficient high-power laser was demonstrated [20] with Yb-doped Lu<sub>2</sub>O<sub>3</sub> ceramic by the same method [21], owing to its excellent optical properties. The crystal was completely transparent and exhibited a low optical loss of less than 0.3% compared with a predicted maximum transmittance at a wavelength of 2.8  $\mu\text{m}$  used for laser emission. The detailed optical characteristics of the ceramics have been described in our previous report [10], where the optical transparency, fluorescence lifetime, and emission cross section were measured at various doping concentrations of Er<sup>3+</sup> ions from 5 to 15 at%. The 11 at.% sample used in this work exhibits best laser performance at a wavelength of 2845 nm.

To investigate the lasing properties, an 8 mm long Er:Lu<sub>2</sub>O<sub>3</sub> ceramics with aperture size of 5×2 mm was pumped with a fiber-coupled laser diode (LD) with a center wavelength of 971 nm in a plane-plane resonator with a cavity length of 24 mm (Fig. 1). For passively  $Q$ -switched operation, monolayer graphene deposited on an antireflection (AR) coated sapphire plate was inserted between the ceramics and an output coupler (OC). The graphene monolayer (Graphene Platform Corp.) was formed by chemical vapor deposition and was confirmed by measurement of the Raman scattering spectrum. The graphene is known to exhibit an initial absorption of 2.3% and a modulation depth higher than 1.5% in the monolayer [22,23]. The total transmittance of the sapphire window and graphene film was approximately 96%. The pump laser was passed through a dichroic mirror (high transmission at 970 nm, high reflection at 2.8  $\mu\text{m}$ ) and was focused on the ceramics as a spot approximately 350  $\mu\text{m}$  in diameter. The optimized transmittance of the OC in CW operation

was 5%. OCs with transmittances of 1, 2, 5, and 8% at 2.8  $\mu\text{m}$ , and a 2.5–3.1  $\mu\text{m}$  band-pass filter were used in the  $Q$ -switched experiment. The ceramics was actively cooled in the crystal holder using water flow at 20  $^{\circ}\text{C}$ . The cavity length of 24 mm was as short as possible using the crystal holder. The output power and temporal waveform were measured using a thermopile power meter (3A, Ophir) and InAs photodetector, respectively. Lasing spectra were also measured using an optical spectrum analyzer (OSA205C, Thorlabs) with a wavelength resolution of *ca.* 0.1 nm.

Figure 2 shows the average output power as a function of the absorbed pump power for CW (OC at 5%) and  $Q$ -switched operation. The absorbed pump power was defined by measurement of the transmitted LD power. Under CW operation without graphene, the output power increased linearly with the pump power to a threshold of 1.3 W, and the maximum output power and slope efficiency were 2.6 W and 26%, respectively. To the best of our knowledge, this is the highest CW output power obtained with an Er:Lu<sub>2</sub>O<sub>3</sub> ceramics laser at 2.8  $\mu\text{m}$ . Under  $Q$ -switched operation, the use of the OC with a transmittance of 5% afforded a highest slope efficiency of 15%, and subsequently efficiencies of 10%, 7%, and 5% for transmittances of 2%, 1%, and 8%, respectively. Stable  $Q$ -switched pulse operation with a monolayer graphene were confirmed by a temporal waveform and a typical waveform with 5% OC and 10.6 W pumping, as shown in Fig. 3. The pulse duration and repetition rate for the results in Fig. 3 were 304 ns and 146 kHz, respectively. This work is the first  $Q$ -switched operation of an Er:Lu<sub>2</sub>O<sub>3</sub> laser using a graphene SA. Figure 4(a) shows the pulse duration and repetition rate plotted as a function of the absorbed pump power in the range of 5.5–11.2 W, where a stable pulse train was obtained. The pulse duration decreased and repetition rate increased with an increase in the pump power. The shortest pulse duration of 247 ns was achieved with a repetition rate of 174 kHz and pumping at 11.2 W. Figure 4(b) shows the pulse energy and peak power as a function of the absorbed pump power. A maximum pulse energy of 9.4  $\mu\text{J}$  and peak power of 33 W were demonstrated under 10.9 W pumping. To the best of our knowledge, these are the shortest pulse duration, highest pulse energy, and highest peak power obtained with a graphene SA at around 3  $\mu\text{m}$  wavelength. Graphene  $Q$ -switching has been reported in the case of Er:Y<sub>2</sub>O<sub>3</sub> ceramics, where the pulse energy and peak power were 2.6  $\mu\text{J}$  and 8.8 W, respectively [15]. Laser output spectra for  $Q$ -

switched operation at various pump powers are shown in Fig. 5. The emission wavelength exhibits a red-shift from 2715 or 2725 to 2845 nm with an increase in the pump power. Such spectral behavior is similar to that under the CW condition we have reported previously [9,10]. A typical intensity profile of the output beam is shown in the inset of Fig. 5. The laser beam quality factors were calculated to be  $M_x^2=1.2$  and  $M_y^2=1.3$ .

In this system, stable pulse trains were observed in the pump power range of 5.5–11.2 W; however, the pulse train became unstable and the average power decreased with an increase in the pump power above 11 W, as shown in Fig. 2. Such unstable behavior at higher pump power is derived from thermal focusing on the gain medium. The effective focal length of the Er:Lu<sub>2</sub>O<sub>3</sub> ceramics due to thermal lens effect can be expressed by [24]

$$f = \frac{\pi K_c w_p^2}{P_{ph} (dn/dT)} \left( \frac{1}{1 - \exp(-\alpha l)} \right), \quad (1)$$

where  $K_c$  is the thermal conductivity of the ceramics,  $w_p$  is the radius of the pump beam,  $P_{ph}$  is the pump power that results in heating,  $\alpha$  is the absorption coefficient, and  $l$  is the length of the ceramics. Assuming a pump power of 11 W pump, and employing Eq. (1) with  $K_c=10.6$  W/mK,  $w_p=175$   $\mu\text{m}$ , and  $P_{ph}=4.4$  W, which is estimated as *ca.* 40% of the pump power [25],  $dn/dT=9.1 \times 10^{-6}$  K<sup>-1</sup>,  $\alpha=8.0$  cm<sup>-1</sup>, and  $l=8$  mm, an effective focal length of  $f=25.3$  mm, which is close to the cavity length (24 mm), is obtained. A focal length that is shorter than the cavity length results in unstable resonance under the condition with pumping at >11 W. For a resonator with a length of 24 mm, the calculated Gaussian mode diameter at the crystal position was *ca.* 320  $\mu\text{m}$ , under the assumption of an effective focal length of 28 mm by 10 W pumping, which was close to the pump beam diameter of 350  $\mu\text{m}$ ; therefore, good spatial mode matching in the gain medium was expected. We have demonstrated passive *Q*-switching without any focusing optics in the resonator and with the cavity mode diameter at the graphene SA estimated as approximately 300  $\mu\text{m}$ .

In an ideal passively *Q*-switched system, the pulse duration  $t_p$  is theoretically estimated by [26]

$$t_p \approx \frac{3.52 \cdot T_R}{\Delta R}, \quad (2)$$

where  $T_R$  is the resonator round-trip time and  $\Delta R$  is the modulation depth of the SA. If the graphene absorption is fully saturated, then the modulation depth will be *ca.* 1.5% [17] and the estimated pulse duration is *ca.* 49 ns in a 24 mm long cavity. The effective modulation

depth is estimated to be 0.3% from the shortest experimentally obtained pulse duration of 250 ns. The pulse energy  $E_p$  is estimated by [26]

$$E_p \approx F_{sat} \cdot A \cdot \Delta R \frac{T_{OC}}{T_{OC} + \alpha}. \quad (3)$$

The saturation fluence of the 11 at% Er-doped Lu<sub>2</sub>O<sub>3</sub> ceramics  $F_{sat}$  is 7.0 J/cm<sup>2</sup> given from an emission cross section of approximately  $1 \times 10^{-20}$  cm<sup>2</sup> at a wavelength of 2845 nm, which was determined in a previous report [10], where  $A$  is the pump spot area,  $T_{OC}$  is the transmittance of the OC, and  $\alpha$  is the round trip loss in the resonator. According to the 0.3% modulation depth of graphene, the round-trip loss estimated from Eq. (3) is *ca.* 6%. This is a relatively low loss considering that it includes the non-saturable loss of graphene and the substrate, Fresnel loss, and diffraction losses. For more power scaling, the pump power must be increased and the cavity length decreased to obtain a higher modulation depth while maintaining the stable resonator condition. In theory, a fully saturated graphene monolayer has the potential to achieve a pulse duration of 49 ns and pulse energy of 101  $\mu$ J in a 24 mm long cavity. A multi-layer graphene film may also improve the pulse energy [15] because the modulation depth increases with the layer number, even though the non-saturable loss will be increased [22]. To reduce the cavity losses, AR coating on the ceramics may be effective in this system. Microchip lasers with dichroic coatings on the pump side of the crystal, and several layers of graphene and partial reflective coatings on the other crystal surface would enable nanosecond pulses with sub-millijoule pulse energies to be obtained [27-29]. In this work, it was confirmed that the graphene film is a suitable SA for mid-IR Er:Lu<sub>2</sub>O<sub>3</sub> lasers, not only for passive  $Q$ -switching but also to achieve passively mode-locking systems [30].

In conclusion, we have demonstrated a passively  $Q$ -switched Er:Lu<sub>2</sub>O<sub>3</sub> ceramics laser using a monolayer graphene SA. Stable pulsed operation with watt-level average power was performed using a compact linear cavity with a length of 24 mm. This is the first successful demonstration of a passively  $Q$ -switched mid-IR Er:Lu<sub>2</sub>O<sub>3</sub> laser using a graphene SA. A maximum pulse energy of 9.4  $\mu$ J and a peak power of 33 W were achieved with a pulse duration of 250 ns. To the best of our knowledge, these are the shortest pulse duration, highest pulse energy, and the highest peak power obtained with a graphene SA in the wavelength region around 3  $\mu$ m. There is thus a possibility to obtain a nanosecond-order pulse with sub-millijoule pulse energy by an increase in the modulation depth of the SA.

### **Acknowledgments**

This work was partially supported by Kakenhi Grants-in-Aid (Nos. 26709072, 15K13386, and 15K04696) from the Japan Society for the Promotion of Science (JSPS) and PRESTO program Grant-in-Aid (No. 15666084) from the Japan Science and Technology Agency (JST).



## References

- 1) P. Werle, F. Slemr, K. Maurer, R. Koormann, R. Mucke, and B. Janker, *Opt. Laser Eng.* **37**, 101 (2002).
- 2) J. L. Boulnois, *Lasers Med. Sci.* **1**, 47 (1986).
- 3) Y. O. Aydin, V. Fortin, R. Vallée, and M. Bernier, *Opt. Lett.* **43**, 4542 (2018).
- 4) V. Fortin, M. Bernier, S. T. Bah, and R. Vallée, *Opt. Lett.* **40**, 2882 (2015).
- 5) S. Tokita, M. Murakami, S. Shimizu, M. Hashida, and S. Sakabe, *Opt. Lett.* **34**, 3062 (2009).
- 6) C. A. Schäfer, H. Uehara, D. Konishi, S. Hattori, H. Matsukuma, M. Murakami, S. Shimizu, and S. Tokita, *Opt. Lett.* **43**, 2340 (2018).
- 7) S. Tokita, M. Murakami, S. Shimizu, M. Hashida, and S. Sakabe, *Opt. Lett.* **36**, 2812 (2011).
- 8) T. Li, K. Beil, C. Kränkel, and G. Huber, *Opt. Lett.* **37**, 2568 (2012).
- 9) H. Uehara, R. Yasuhara, S. Tokita, J. Kawanaka, M. Murakami and S. Shimizu, *Opt. Express* **25**, 18677 (2017).
- 10) H. Uehara, S. Tokita, J. Kawanaka, D. Konishi, M. Murakami, S. Shimizu, and R. Yasuhara, *Opt. Express* **26**, 3497 (2018).
- 11) L. Wang, H. Huang, D. Shen, J. Zhang, and D. Tang, *Appl. Sci.* **8**, 801 (2018).
- 12) M. Fan, T. Li, S. Zhao, G. Li, H. Ma, X. Go, C. Kränkel, and G. Huber, *Opt. Lett.* **41**, 540 (2016).
- 13) M. Fan, T. Li, S. Zhao, G. Li, X. Gao, K. Yang, D. Li, and C. Kränkel, *Photon. Res.* **4**, 181 (2016).
- 14) M. Fan, T. Li, G. Li, H. Ma, S. Zhao, K. Yang, and C. Kränkel, *Opt. Lett.* **42**, 286 (2017).
- 15) X. Guan, L. Zhan, Z. Zhu, B. Xu, H. Xu, Z. Cai, W. Cai, X. Xu, J. Zhang, and J. Xu, *Appl. Opt.* **57**, 371 (2018).
- 16) C. Wei, X. Zhu, F. Wang, Y. Xu, K. Balakrishnan, F. Song, R. A. Norwood, and N. Peyghambarian, *Opt. Lett.* **38**, 3233 (2013).
- 17) C. Li, J. Liu, S. Jiang, S. Xu, W. Ma, J. Wang, X. Xu, and L. Su, *Opt. Mater. Express* **6**, 1570 (2016).
- 18) Z. Y. You, Y. Wang, Y. J. Sun, J. L. Xu, Z. J. Zhu, J. F. Li, H. Y. Wang, and C. Y. Tu, *Laser Phys. Lett.* **14**, 045810(2017).
- 19) H. Nie, P. Zhang, B. Zhang, K. Yang, L. Zhang, T. Li, S. Zhang, J. Xu, Y. Hang, and J. He,

- Opt. Lett. **42**, 699 (2017).
- 20) H. Nakao, T. Inagaki, A. Shirakawa, K. Ueda, H. Yagi, T. Yanagitani, A. A Kaminskii, B. Weichelt, K. Wentsch, M. A. Ahmed, and T. Graf, Opt. Mater. Express **4**, 2116 (2014).
  - 21) T. Yanagida, Y. Fujimoto, H. Yagi, and T. Yanagitani, Opt. Mater. **36**, 1044 (2014).
  - 22) Q. Bao, H. Zhang, Y. Wang, Z. Ni, Y. Yan, Z. X. Shen, K. P. Loh, and D. Y. Tang, Adv. Funct. Mater. **19**, 3077 (2009).
  - 23) R. R. Nair, P. Blake, A. N. Grigorenko, K. S. Novoselov, T. J. Booth, T. Stauber, N. M. R. Peres and A. K. Geim, Science **320**, 1308 (2008).
  - 24) M. E. Innocenzi, H. T. Yura, C. L. Fincher, and R. A. Fields, Appl. Phys. Lett. **56**, 1831 (1990).
  - 25) M. Pollnau, IEEE J. Quantum Electron. **39**, 350 (2003).
  - 26) G. J. Spuhler, R. Paschotta, R. Fluck, B. Braun, M. Moser, G. Zhang, E. Gini, and U. Keller, J. Opt. Soc. Am. B **16**, 376 (1999).
  - 27) H. Sakai, H. Kan, and T. Taira, Opt. Express **16**, 19891 (2008).
  - 28) X. Guo, S. Tokita, and J. Kawanaka, Opt. Lett. **43**, 459 (2018).
  - 29) X. Guo, K. Hamamoto, S. Tokita, and J. Kawanaka, Las. Phys. Lett. **15**, 105001 (2018).
  - 30) H. Xue, L. Wang, W. Zhou, H. Wang, J. Wang, D. Tang, and D. Shen, Appl. Sci. **8**, 1155 (2018).

## Figure Captions

**Fig. 1.** Schematic of the setup for a passively  $Q$ -switched Er:Lu<sub>2</sub>O<sub>3</sub> ceramics laser using a graphene SA.

**Fig. 2.** Average output power of the Er:Lu<sub>2</sub>O<sub>3</sub> ceramics laser as a function of absorbed pump power for CW operation (OC 5%) and graphene  $Q$ -switched operation (OC transmittances of 1, 2, 5, and 8%).

**Fig. 3.** Typical output temporal waveform of the graphene  $Q$ -switched Er:Lu<sub>2</sub>O<sub>3</sub> ceramics laser under 10.6 W pumping with 5% OC. Inset: temporal waveform of a pulse in the pulse train.

**Fig. 4.** (a) Pulse duration and repetition rate as a function of absorbed pump power. (b) Pulse energy and peak power as a function of the absorbed pump power of the graphene  $Q$ -switched Er:Lu<sub>2</sub>O<sub>3</sub> ceramics laser with 5% OC. Stable pulse train was observed in the pump power range of 5.5–11.2 W.

**Fig. 5.** Laser output spectra for the graphene  $Q$ -switched Er:Lu<sub>2</sub>O<sub>3</sub> ceramics laser at various pump powers. Inset: typical intensity profile of the output beam.

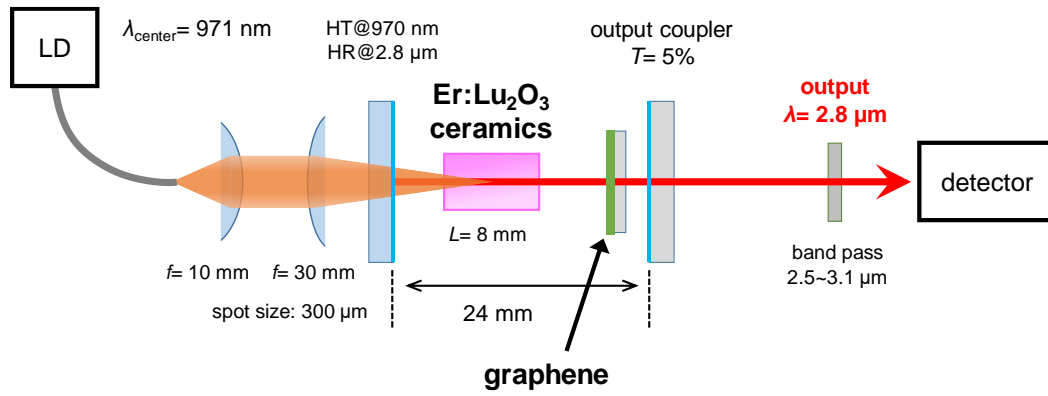


Fig. 1

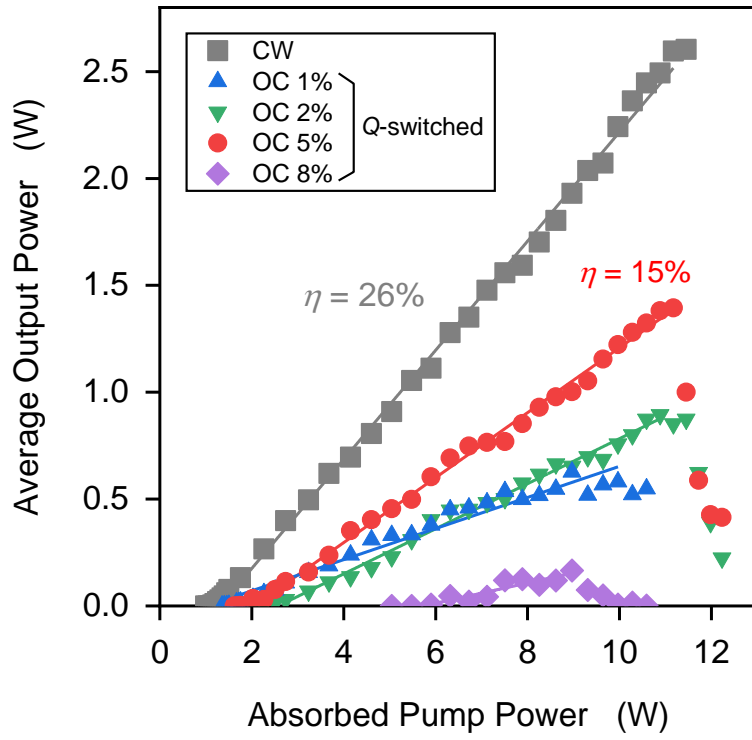


Fig. 2

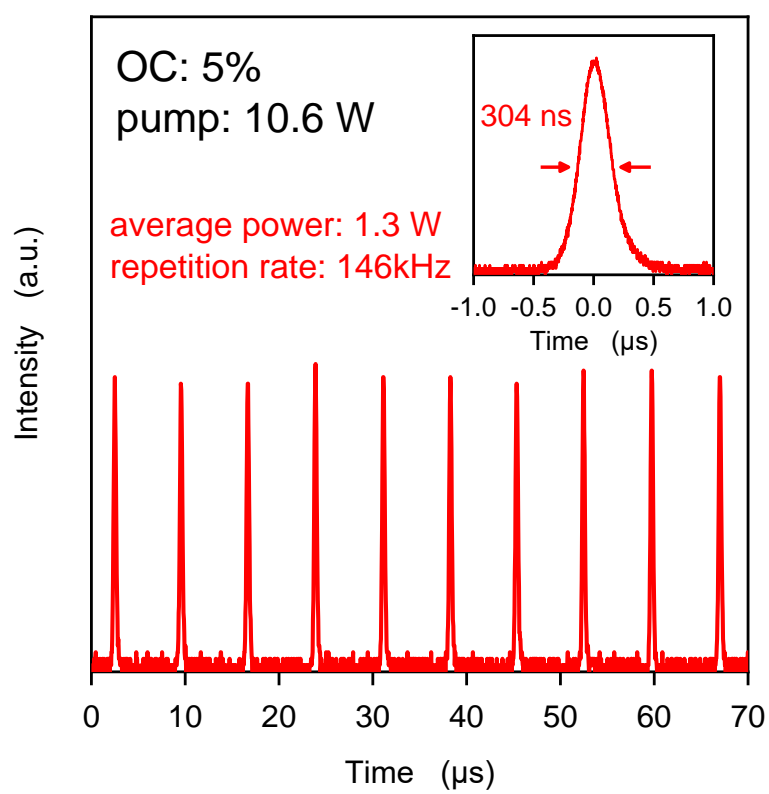


Fig. 3

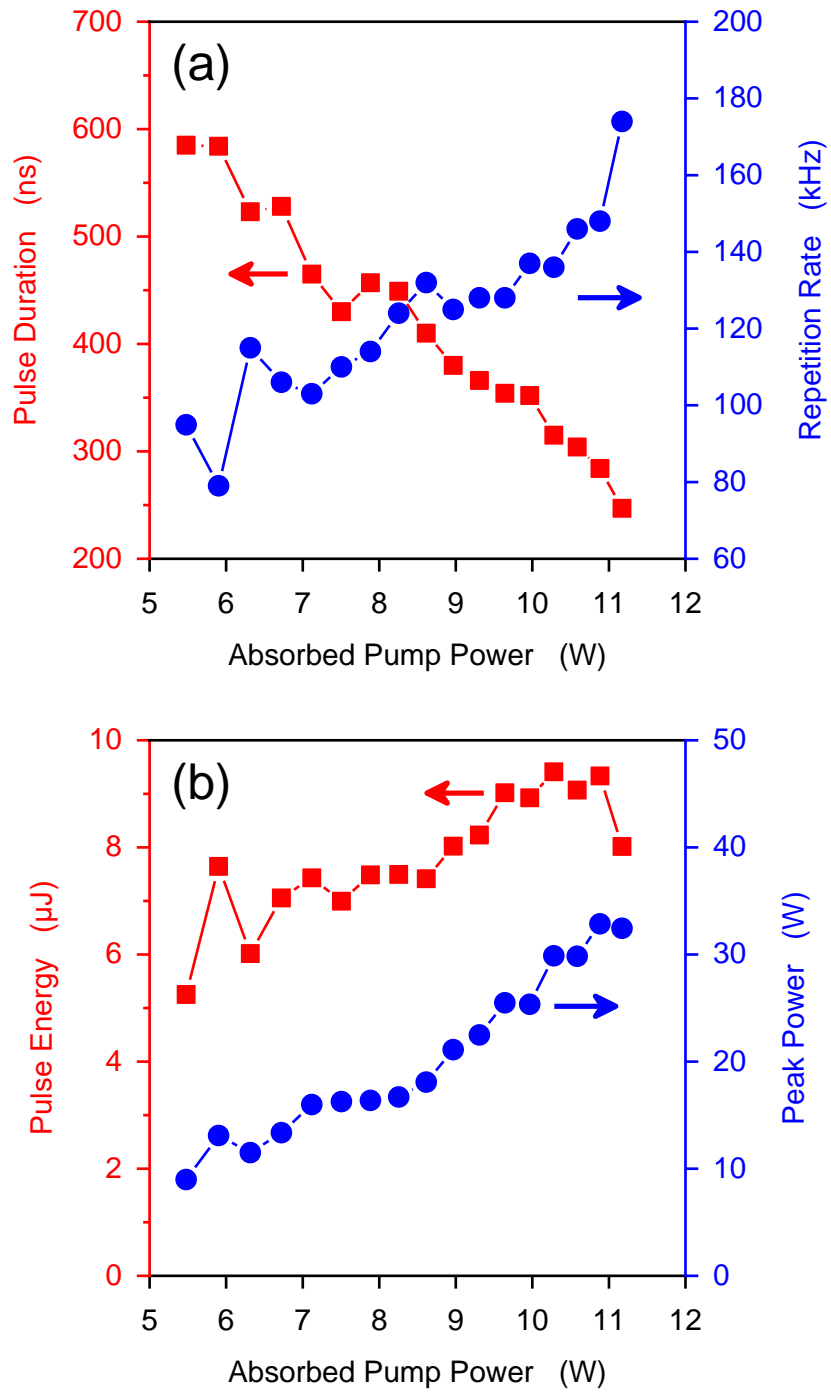


Fig. 4

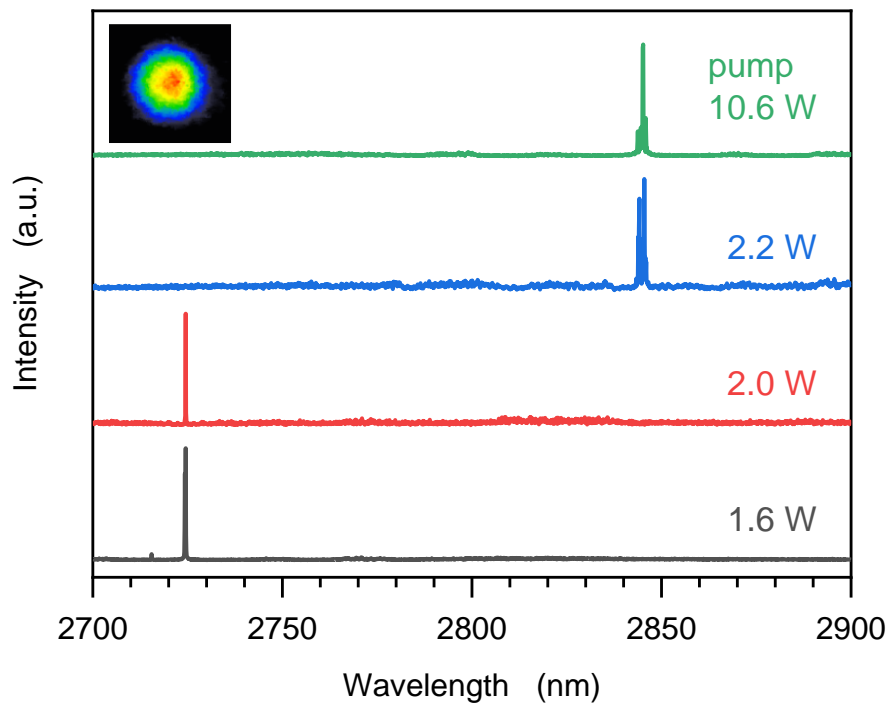


Fig. 5